



RESEARCH ARTICLE

**EVALUATION OF THE MONITORING OF SURFACE DEFORMATIONS IN OPEN-PIT
MINES WITH SENTINEL-1A SATELLITE RADAR DATA**

Bekir POYRAZ^{1*}, Yavuz GÜL², Fatih POYRAZ³

¹Sivas Cumhuriyet University, Division of Mining Engineering, bpoyraz@cumhuriyet.edu.tr,
ORCID: 0000-0003-2832-4632

²Sivas Cumhuriyet University, Engineering Faculty, Civil Engineering, ygul@cumhuriyet.edu.tr,
ORCID: 0000-0002-2969-577X

³Sivas Cumhuriyet University, Engineering Faculty, Geomatics Engineering, fpoyraz@cumhuriyet.edu.tr,
ORCID: 0000-0001-9471-7261

Receive Date: 28.07.2023

Accepted Date: 25.08.2023

ABSTRACT

Accidents and loss of life can occur in surface mines due to large mass displacements (landslides). In order to prevent these irreversible situations, it is very important to identify displacements in advance or to take necessary measures by obtaining early warning signs. Within the scope of this study, satellite radar images (SAR, Synthetic Aperture Radar) obtained from the European Space Agency (ESA) Sentinel-1A satellite were used to reveal the traceability and monitoring sensitivity of deformations and possible mass displacements in the dump area of a mining operation. The results obtained from 2 Global Positioning Systems (GPS) installed in the field were compared with the results obtained from satellite radar data and their compatibility with each other was evaluated. When the horizontal/vertical velocity values obtained by decomposing the Sentinel-1A ascending and descending satellite line of sight (LOS, Line Of Sight) velocities were compared with the horizontal/vertical velocity values of GPS, the results were statistically equal. GPS-based vertical velocities were -131.5 mm/year at GPS1 and -20.7 mm/year at GPS2, while Sentinel-1A-based velocities were -94.5 mm/year at GPS1 and -7.8 mm/year at GPS2. While both GPS and satellite-based vertical deformations show the same direction (in the form of subsidence), the deformation velocity values obtained from satellite radar data are lower than GPS results. Horizontal deformations obtained with satellite radar data could not be determined in the north/south direction due to satellite orbital motions, while they could be partially determined in the east/west direction. GPS-based east/west horizontal velocities were +2.8 mm/year in GPS1 and insignificant velocity was found in GPS2. Satellite-based east/west horizontal velocity values were +6.8 mm/year at GPS1 and +8.4 mm/year at GPS2.

Keywords: GPS, InSAR, LOS, SBAS, Sentinel-1A, Surface mining

1. INTRODUCTION

Today, deformation determination studies in open pit mines are generally carried out on a point basis and landslide risk is tried to be determined according to the general movements of these points. If the locations of the points are not within the deformation zones, it is assumed that there is no risk in the study area [1]. This situation prevents measures from being taken against possible landslides. Discontinuity and stress directions change due to the ongoing excavation works in mining operations. When determining deformation areas, not only certain areas but the entire working area and its surroundings should be considered as possible deformation areas. Therefore, deformation monitoring studies should be areal rather than point-based and should cover the entire study area.

The two best methods for monitoring deformation on an areal basis are remote sensing and aerial photogrammetry. In recent years, the Interferometric Synthetic Aperture Radar (InSAR) method, which utilizes satellite data to determine surface deformations and movements over vast areas, has emerged as a prominent technique [2]. In this method, delays in the signals reflected and returned from the satellite are detected, enabling the generation of high-resolution images through signal processing.

While point-based deformations can be monitored very effectively with GPS, deformations over large areas can be monitored using satellite radar data [3-5]. GPSs are capable of determining the three-dimensional position of points with mm accuracy. While GPSs can be easily used to monitor slow landslides in small areas, monitoring large areas requires the tracking of a large number of points. On the other hand, the InSAR method is capable of reliably measuring daily or longer-term displacements in the earth's surface with mm accuracy, using satellite radar imagery to monitor deformations and tectonic movements over extensive areas [3,6-10]. These two methods have their respective advantages and disadvantages. The most important shortcomings of this system are the necessity to select an appropriate model to correct ionospheric errors in GPS measurements and the fact that data acquisition is limited to the point of installation [11]. When continuously monitoring a large number of points with GPS networks, high costs can be incurred [10]. However, the biggest advantage of GPS measurement is that it provides mm-accurate values for east/west, north/south, and up/down directions on a point-by-point basis [12]. On the other hand, the InSAR method offers significant advantages such as monitoring large areas, high temporal resolution, and all-weather monitoring [13]. Nevertheless, the main disadvantages of this method include limitations in deformation tracking due to satellite transit times [5], the impact of atmospheric effects on measurement results [13,14], and the inability to determine north/south direction deformations [5,8-10,15,16]. Considering these factors together, it is suggested that more accurate surface displacement estimates can be achieved by using GPS and InSAR methods together, providing results with both high temporal and spatial resolution [2,8]. Additionally, by utilizing both methods, the disadvantages associated with point-based tracking and satellite transit times are expected to be overcome.

Within the scope of this study, satellite radar data (SAR, Synthetic Aperture Radar), and GPS data were utilized to detect horizontal and vertical deformations in a specific region at a mine site. Simultaneously with the provision of SAR data, 2 GPS units were installed in the field, and measurements were conducted. Horizontal and vertical deformation velocity values determined from

both SAR and GPS measurements were compared, revealing the similarities and differences between them.

2. MATERIAL AND METHODOLOGY

The horizontal and vertical deformation rates determined from Sentinel-1A satellite SAR data, considering the date of installation of the GPSs, were determined by taking into account the nearest Distributed Scatterer (DS) value at the points where the GPSs were installed. These results were then compared with the horizontal and vertical deformation velocities obtained from the GPSs.

2.1. Study Area

The studied area is the Kalburçayırı coal open-pit area where the coal needs of the Kangal Thermal Power Plant are met (Figure 1). The operation site is located within the borders of the Kangal district of Sivas province, Turkey. Kalburçayırı, situated in the southern part of the district center and approximately 30 km away from the district, features coal deposits of 7 m thickness in two seams. The cover on the upper vein measures 42 m in thickness, while an intermediate cover of 20 m separates the two veins. The coal is accompanied by limestone, clayey limestone, and marl as side rocks. The area comprises small hills, presenting a high plateau appearance. Due to erosions, the south of the area is more hilly than the north [17].

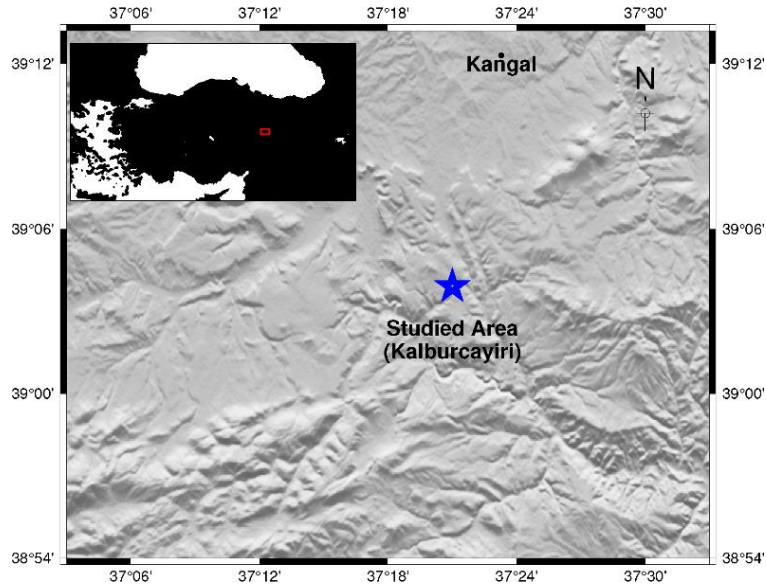


Figure 1. Studied area.

2.2. Methodology And Data Set

In line with the workflow plan given in Figure 2, the studies outlined below were carried out.

- Installation of 2 GPS units in the field to compare whether satellite radar imagery-based studies produce reliable results.
- Providing satellite radar images in descending and ascending orbit from Sentinel-1A satellite of the European Space Agency (ESA).
- Determination of horizontal and vertical deformation velocities by decomposing method from deformation velocities in the satellite line-of-sight (LOS) direction obtained from SAR data,
- Comparison of horizontal and vertical deformation velocity values determined from Sentinel-1A satellite radar data with horizontal and vertical deformation velocity values estimated from GPS results.

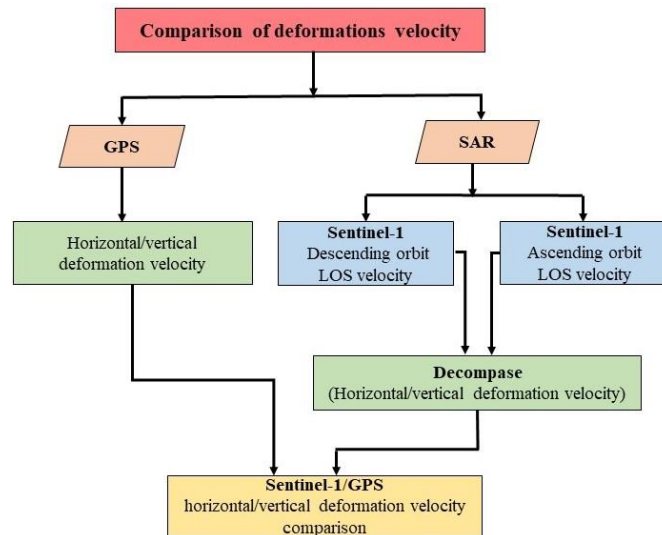


Figure 2. Work flow plan.

Within the scope of the study, 19 SAR data of the Sentinel 1A (IW, Interferometric Wide Swath Mode) satellite in descending (10) and ascending (9) orbits were used, taking into account the data acquisition date of the GPS installed in Kangal Kalburçayırı field (June 01, 2022 - October 31, 2022). The satellite image data set used is given in Table 1.

Table 1. Time range and image numbers of the satellite radar data.

Sentinel-1A				
	Image ID	Date	Frame	Product Modes
Ascending	1	20220715	116	IW
	2	20220727	116	IW
	3	20220808	116	IW
	4	20220820	116	IW
	5	20220901	116	IW
	6	20220913	116	IW

	7	20220925	116	IW
	8	20221007	116	IW
	9	20221019	116	IW
Descending	1	20220709	21	IW
	2	20220721	21	IW
	3	20220802	21	IW
	4	20220814	21	IW
	5	20220826	21	IW
	6	20220907	21	IW
	7	20220919	21	IW
	8	20221001	21	IW
	9	20221013	21	IW
	10	20221025	21	IW

2.3. SAR Calculations

For the Sentinel-1A satellite, 9 ascending orbital radar images from July 15, 2022, to October 19, 2022, and 10 descending orbital radar images from July 9, 2022, to October 25, 2022, are used as datasets in Table 1. The deformation velocity values in the LOS direction were determined by GMTSAR [18,19], StaMPS/MTI (Stanford Method for Persistent Scatterers) [20] programs, and SBAS technique, and the interferogram pairs are shown in Figure 3. GMTSAR is an open-source InSAR processing system based on Generic Mapping Tools (GMT).

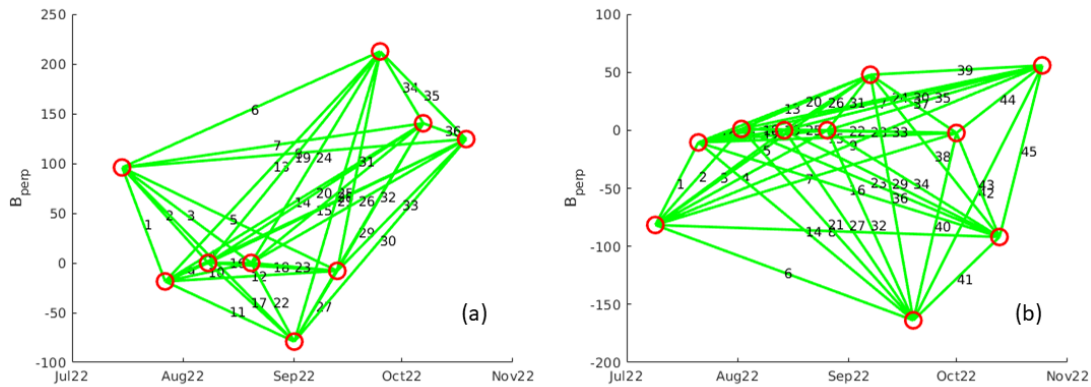


Figure 3. Spatial and temporal distribution of the Sentinel-1A image relative to SBAS (Green lines indicate interferogram pairs). a) 116 track numbers ascending. b) 21 track numbers descending.

The MineSAR program was used for the determination and detailed evaluation of the horizontal and vertical deformation velocities of the DS points around the GPS locations using the decomposing method. MineSAR software supported by the Small and Medium Enterprises Development Organization of Turkey (KOSGEB) within the scope of the R & D, Innovation and Industrial Application Support Program was developed by Geomine R&D Software Company. With MineSAR

software, a limited region can be encircled from the entire deformation area and the DSs at that location can be seen.

LOS deformation velocities are converted to horizontal and vertical directions using the following equations in MineSAR software. Surface deformations are expressed as $V=(V_E, V_N, V_{UP})^T$ in three dimensions in the east, north, and up directions. The transformation of the surface displacement vector to the V_{LOS} satellite line of sight is written as in Eq. 1. In Eq. 1, V_{LOS} , s , and V are the LOS displacement, satellite unit vector, and three-dimensional surface displacement vectors, respectively. Eq. 2 shows the satellite unit vector in detail. For ascending and descending transitions, α_h in Eq. 2 is the angle of heading, and θ is the angle of incidence [3,21,22]. In the last stage, the LOS displacement values of the descending and ascending satellites were converted into east and up components using Eq. 3 [23].

$$V_{LOS}=s^T.V \quad (1)$$

$$s=(-\cos\alpha_h\sin\theta \quad \sin\alpha_h \sin\theta \quad \cos\theta)^T \quad (2)$$

$$\begin{pmatrix} -\cos(\alpha_{ASC}) & \sin(\alpha_{ASC}) \cos(\delta_{ASC}) \\ -\cos(\alpha_{DSC}) & \sin(\alpha_{DSC}) \cos(\delta_{DSC}) \end{pmatrix} \begin{pmatrix} V_{UP} \\ V_{EW} \end{pmatrix} = \begin{pmatrix} V_{LOS,ASC} \\ V_{LOS,DSC} \end{pmatrix} \quad (3)$$

In Eq. 3, for ascending and descending satellites, α_{ASC} , α_{DSC} denotes the angles of heading, and δ_{ASC} , $\cos(\delta_{DSC})$ denotes the angles of incidence (Figure 4). V_{UP} is the velocity for the up component, V_{EW} is the velocity for the east component, $V_{LOS,ASC}$ is the velocity in the ascending satellite LOS direction, $V_{LOS,DSC}$ is the velocity in the descending satellite LOS direction. Vertical and horizontal deformation velocity maps are given in Figures 5 and 6.

From the LOS data, vertical up/down and east/west horizontal displacements can be detected, while north/south horizontal displacements cannot be detected due to the satellite's orbit motion. [2,9,15,16].

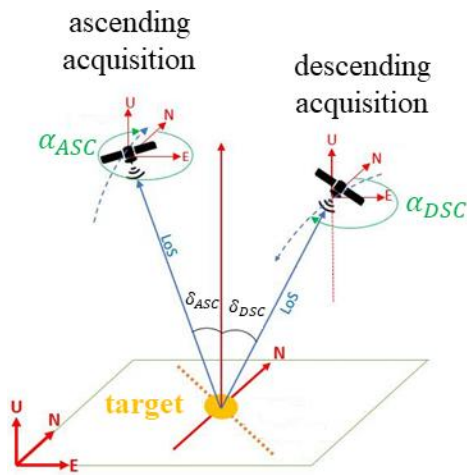


Figure 4. Schematic overview of the imaging geometry of a satellite in ascending and descending orbits [24].

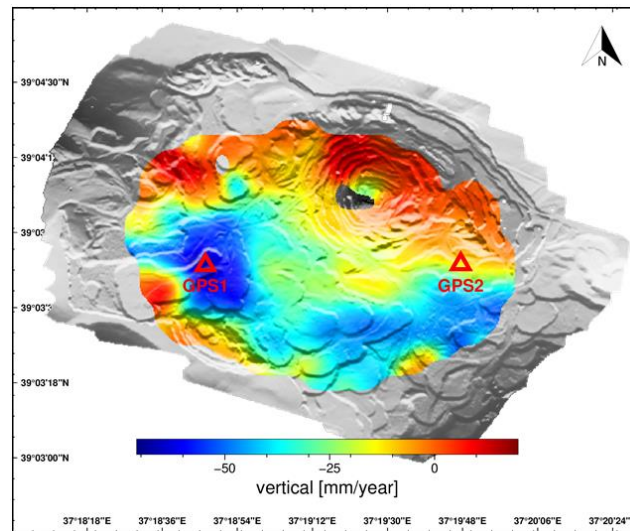


Figure 5. Spatial distribution maps of vertical deformation velocities.

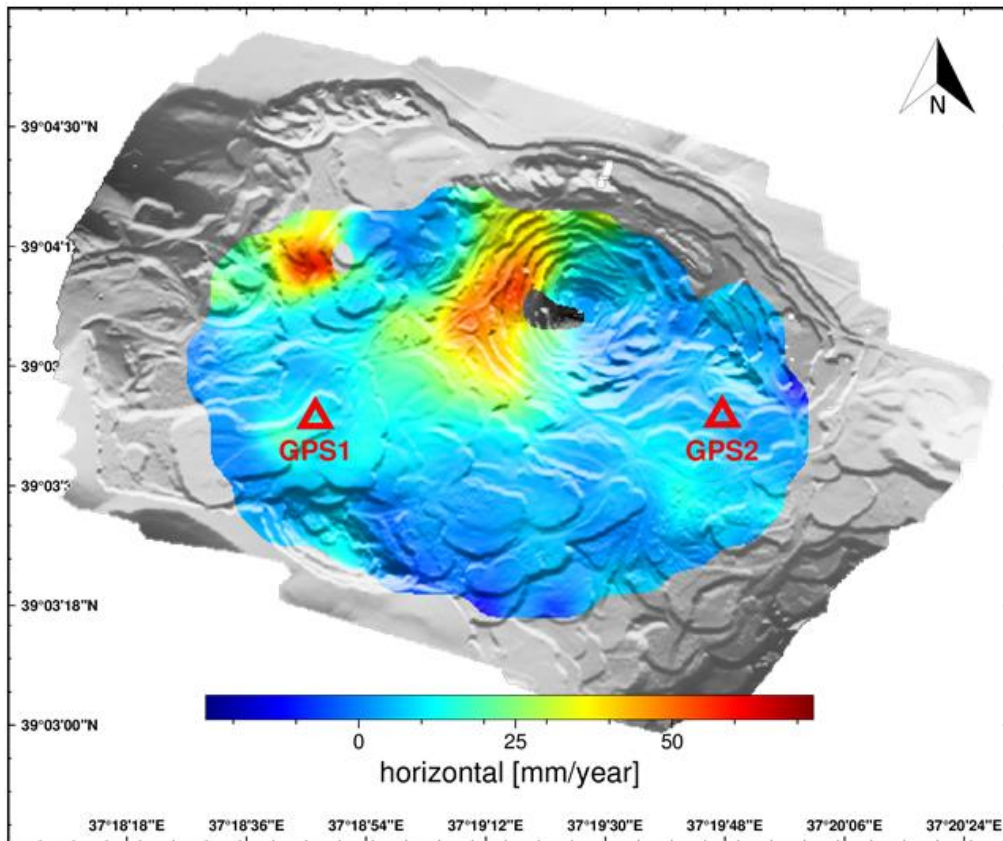


Figure 6. Spatial distribution maps of horizontal deformation velocities.

In order to compare the horizontal/vertical deformation velocities determined from Sentinel-1A satellite radar data with the horizontal/vertical deformation velocities obtained from GPS1 and GPS2 data, the DS points closest to the point where GPS1 and GPS2 were installed were considered (Figure 7).

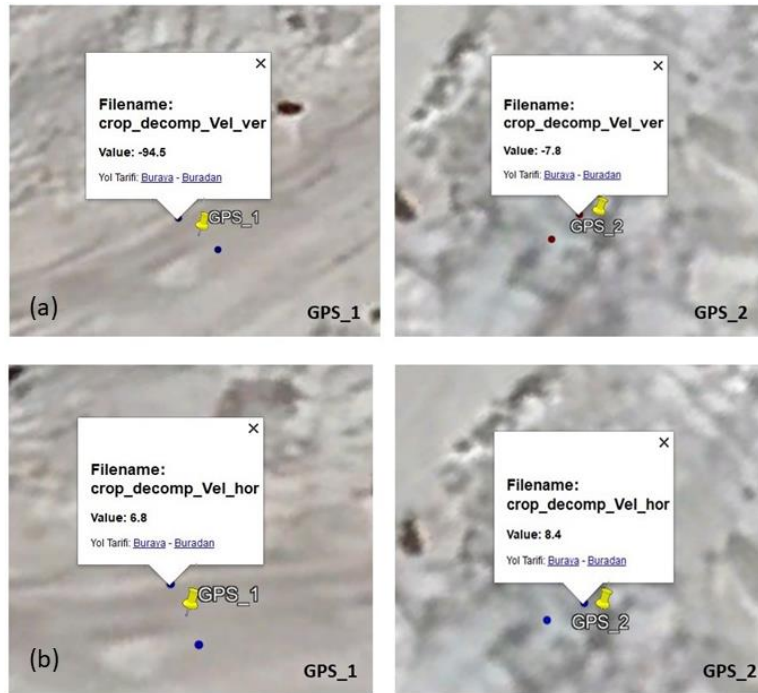


Figure 7. DS point nearest to GPS point. a) vertical deformation. b) horizontal deformation.

Velocity values of DS points in horizontal and vertical directions were calculated according to Eq. 3. The standard deviation values of the DS points in horizontal and vertical directions were obtained by applying the error propagation rule to Eq. 3 (Table 2). The reason for choosing one DS point closest to the GPS points is that the error propagation rule can only be applied to the first measurements when calculating the standard deviation values of the DS points. Since the error propagation rule is applied to the first measurement values, the closest DS point is chosen instead of the average of the DSs around the GPS point.

As a result of the decomposition process according to Eq. 3, the velocity values of the up and east components were estimated, while the standard deviation values were obtained using the "Error propagation rule." It is inevitable that inaccuracies in the measurements will result in inaccuracies in the calculated magnitudes. The process of determining the effects of errors in the measurements on the functions calculated from these measurements is carried out according to the Error Propagation Rule. We assume that the measurements L_1 , L_2 , and L_3 , with known variances and covariances, have x and y functions (Eq. 4 and 5) as follows,

$$x = g(L_1, L_2, L_3) \quad (4)$$

$$y = h(L_1, L_2, L_3) \quad (5)$$

The effect of errors in the measurements on the x, y functions can be determined by taking the differential of these functions with respect to the measurements (Eq. 6 and 7). The error propagation rule applies only to the first measurements [25].

$$dx = \frac{\partial g}{\partial L_1} dL_1 + \frac{\partial g}{\partial L_2} dL_2 + \frac{\partial g}{\partial L_3} dL_3 \quad (6)$$

$$dy = \frac{\partial h}{\partial L_1} dL_1 + \frac{\partial h}{\partial L_2} dL_2 + \frac{\partial h}{\partial L_3} dL_3 \quad (7)$$

Table 2. The amount of horizontal/vertical deformation at the DS point nearest to GPS1 and GPS2

	GPS1 point (mm/year)	std	GPS2 point (mm/year)	std
Vertical deformation	-94.5	18.1	-7.8	5.4
Horizontal deformation	6.8	17.0	8.4	5.2

Considering the DSs at the closest distance to the GPS points, the vertical deformation rate at the GPS1 location was -94.5 mm/year and the horizontal deformation rate was +6.8 mm/year, while the vertical deformation rate at the GPS2 location was -7.8 mm/year and the horizontal deformation rate was +8.4 mm/year.

2.4. GPS Calculations

In order to compare the horizontal and vertical deformation velocity values obtained from SAR data, 2 "Z-MAX THALES" brand GPS devices were installed within the boundaries shown in Figure 8 in the area we call the deformation area. GPS devices have been continuously powered by solar panels and batteries. The deformation area has been tracked with GPS devices for approximately 4 months.

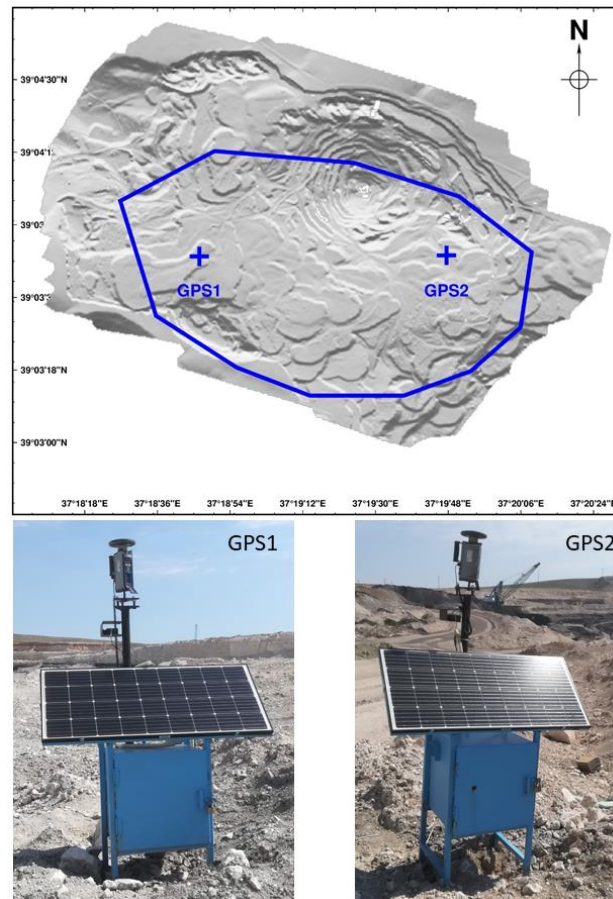


Figure 8. GPS's installed in the field.

GPS1 and GPS2 devices were installed in the field on June 01, 2022. The measurement results were evaluated on the website of the Geodetic Research Center of Canada [26], and the horizontal and vertical positions of the GPSs on the earth's surface were determined. Horizontal and vertical deformation velocity values were estimated from the time series (Figure 9) produced with the help of these data. There were interruptions in the time series given in Figure 9, due to a lack of data. This is due to the low data storage capacity of the device in question. However, as seen in Figure 9, this lack of data did not affect the general trend.

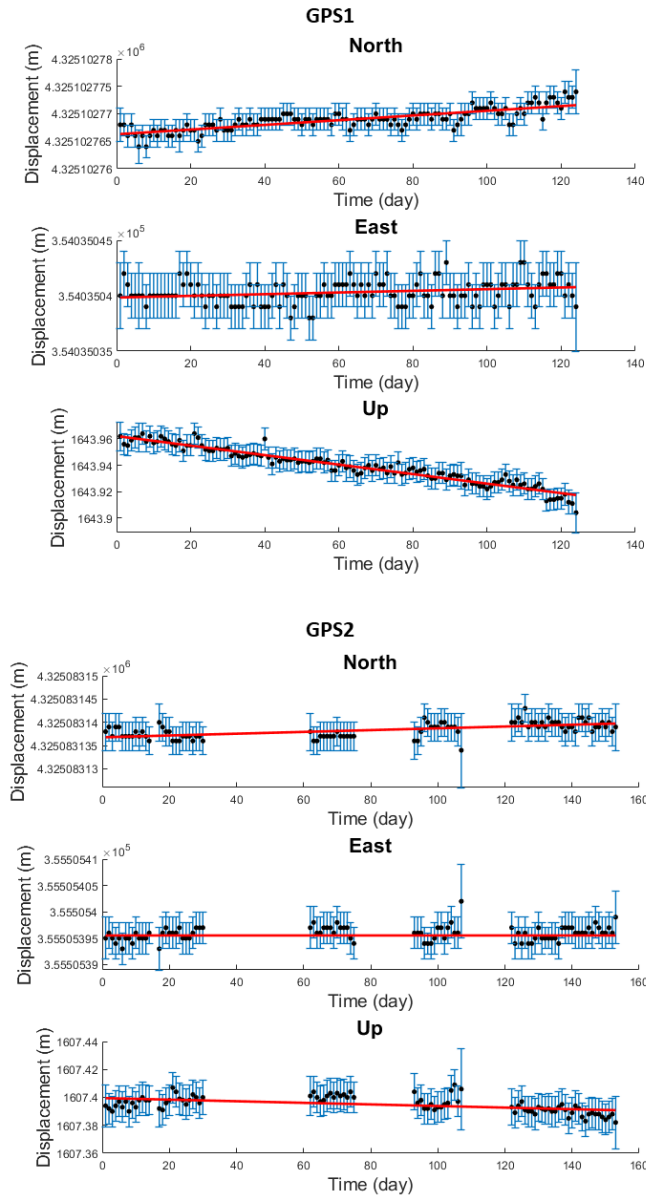


Figure 9. Time series for GPS1 and GPS2 points.

The velocity values obtained from the time series of GPS1 and GPS2 were analyzed using a t-test (at $\alpha = 0.05$ confidence interval, t-test value; 1.9796 for GPS1 and 1.9876 for GPS2). Significant velocity values were determined and the obtained numerical quantities are presented in Table 3.

Table 3. GPS horizontal/vertical deformation estimated velocity values.

	GPS1				GPS2			
	V (mm/year)	SV _{Std}	t-test	Decision	V (mm/year)	SV _{Std}	t-test	Decision
North	15.6	1.05	14.83	significant	7.0	0.93	7.60	significant
East	2.8	0.95	2.89	significant	1.3	0.91	1.42	unsignificant
Up	-131.5	3.27	40.28	significant	-20.7	3.64	5.70	significant

- Vertical deformations in the form of collapse were determined as -131.5 mm/year at GPS1 and -20.7 mm/year at GPS2.
- For the horizontal deformations in the east/west direction, the velocity value was +2.8 mm/year at the GPS1 point, while unsignificant velocity value was found at the GPS2 point.
- The horizontal deformation values in the north/south direction were +15.6 mm/year at GPS1 and +7.0 mm/year at GPS2.

Based on the t-test results, the velocities in the directions of North, East, and Up at GPS1, and North and Up at GPS2 were found to be significant. However, the velocity value in the east/west direction at GPS2 was found to be unsignificant.

3. DISCUSSIONS

Horizontal/vertical velocity values were determined by decomposing Sentinel-1A data. F-test and t-test analyses were performed to determine whether the horizontal/vertical velocity values of Sentinel-1A and GPSs can be considered equal. Firstly, the equality of variances was checked with the F-test, and accordingly, the variance of the difference to be used in the t-test was calculated. The results obtained are presented in Table 4.

Table 4. GPS and Sentinel-1A horizontal/vertical deformation velocity comparison.

ID	Vertical deformation							F test		t-test	
	GPS (mm/year)			Sentinel-1A (mm/year)			Velocity difference	GPS1 F limit :2.086	GPS2 F limit :3.282	GPS1 t limit :2.364	GPS2 t limit :2.322
	n	V	std	n	V	std	Vd	F test	Decision	t-test	Decision
GPS1	124	-131.5	3.27	9	-94.5	18.1	-37	2.22	not equal	2.01	Equal
GPS2	89	-20.7	3.64	9	-7.8	5.4	-12.9	4.49	not equal	1.98	Equal
ID	Horizontal deformation							F test		t-test	
	GPS (mm/year)			Sentinel-1A (mm/year)			Velocity difference	GPS1 F limit :2.086	GPS2 F limit :2.117	GPS1 t limit :2.365	GPS2 t limit :2.364
	n	V	std	n	V	std	Vd	F test	Decision	t-test	Decision
GPS1	124	2.8	0.95	9	6.8	17.0	4.0	23.24	not equal	0.23	Equal

GPS2	89	1.3	0.91	9	8.4	5.2	7.1	3.30	not equal	1.34	Equal
-------------	----	------------	------	---	------------	-----	-----	------	-----------	------	--------------

**n: Number of measures; V: LOS velocity (mm/year); std: Standard deviation*

As a result of the comparisons made by considering the horizontal/vertical velocity values given in Table 4. the following findings were made.

Although the variances of the satellite and GPS-based velocities obtained at GPS1 and GPS2 points for vertical and horizontal deformations were not equal, the velocity values were found to be equal according to the statistical analysis results. Therefore, the velocities obtained can be considered equal.

GPS-based vertical velocities were -131.5 mm/year at GPS1 and -20.7 mm/year at GPS2, while Sentinel-1A-based velocities were -94.5 mm/year at GPS1 and -7.8 mm/year at GPS2. While GPS and satellite-based vertical deformations show the same direction (in the form of subsidence), the deformation velocity values obtained from satellite radar data are lower at both GPS1 and GPS2 points compared to GPS results. Similar results were observed in studies [9]. It is stated that the horizontal/vertical velocity values obtained from satellite radar images are lower than the velocity values obtained with GPS. This study also presents similar findings. The difference in deformation velocity magnitudes is believed to be due to the fact that Distributed Scatterers (DS) could not be found at the exact GPS points, and therefore, the deformation velocity value at the DS point closest to the GPS point was taken into account. However, the use of fewer data and larger standard deviations when estimating velocity values from SAR data compared to GPS (Table 4) is considered to be an important factor in the different results. The number of data for velocity estimation is 124 for GPS1, 89 for GPS2, and only 9 for Sentinel-1A. Moreover, while the standard deviation values for GPS are around 3.5 mm/year, the standard deviation of SAR data reaches up to 18 mm/year.

Horizontal deformations obtained with satellite radar data could not be determined in the north/south direction due to satellite orbital motions, while they could be partially determined in the east/west direction. These values were determined as +2.8 mm/year at the GPS1 point, and insignificant velocity was found at the GPS2 point. Additionally, the horizontal deformation values in the east/west direction were +6.8 mm/year at the GPS1 point and +8.4 mm/year at the GPS2 point.

Although north/south deformation velocities of +15.6 mm/year at GPS1 and +7.0 mm/year at GPS2 were determined based on GPS, these velocities/movements could not be detected with satellite-based data. In studies on the subject, it is stated that approximately 7% to 11% of the deformations in the north/south direction can be determined by the decomposition method from satellite radar data [2,9]. In light of this information and considering the small of number values, the reason for not obtaining a satellite-based north/south directional result can also be explained. This situation is confirmed in the literature.

According to these determinations; since the horizontal/vertical deformation velocity values obtained from GPS and Sentinel-1A data are statistically equal according to the t-test, the results are compatible. The deformation directions determined from both GPS and SAR data are the same. In this study, vertical and horizontal deformations obtained using GPS and satellite radar data gave similar results to previous studies [2,3,9,27-29].

4. CONCLUSIONS AND RECOMMENDATIONS

In this study, the dump site of a coal mine was selected as the study area. Horizontal and vertical deformation velocities in the area were determined using data from the Sentinel-1A satellite over a specific time interval. To validate and compare the satellite radar data, GPS devices were installed at 2 points within the deformation area, and deformations were measured over approximately 4 months. The horizontal and vertical deformations determined by both SAR images and GPS data were compared and the results are given below.

The directions of horizontal and vertical deformations determined from GPS and Sentinel-1A data are consistent. Velocity values are consistent according to the t-test. Although the vertical and horizontal deformation velocities obtained by the decomposition method based on Sentinel-1A are lower than the GPS-based velocities, they generally show the same direction (in the form of collapse). These results are consistent with the literature.

Although a north/south directional movement was determined based on GPS, these velocities/movements could not be detected with satellite-based data. In studies on the subject, it is stated that approximately 10% of the north/south deformations can be determined using satellite radar data. Considering that the numbers are very small, it is an expected result that a satellite-based north/south deformation could not be obtained. This situation also supports the observation in the previous point.

Satellite-based velocity values were found to be lower than GPS-based velocity values. This is thought to be due to the use of fewer data and larger standard deviations when estimating velocity values from SAR data compared to GPS. On the other hand, despite the differences in magnitudes, the deformation directions obtained from GPS data and the directions obtained from SAR data were found to be the same.

When the above-mentioned points are evaluated as a whole, it is useful to consider the following recommendations and suggestions.

In satellite radar-based deformation monitoring, a significant problem is that deformation detection times are limited to the acquisition dates of satellite imagery. Deformations that occur between satellite passes cannot be monitored until the next acquisition. The most crucial advantage of GPS over satellite-based techniques is its capability to determine horizontal deformations in the north/south direction. However, since GPS allows only point-based assessments, monitoring large areas by establishing GPS networks can be costly and workforce.

The comparison of GPS and Sentinel-1A velocity values was statistically equal. The velocity magnitudes determined by the InSAR/SBAS technique were lower than those determined by GPS. Nevertheless, the InSAR/SBAS technique provided consistent results in terms of deformation directions and continuity. The study's results suggest that the InSAR/SBAS technique can be effectively used to monitor deformations in mining areas with sufficient sensitivity for early warning purposes.

With the combination of the InSAR technique and GPS systems, it is thought that the deformations can be monitored more effectively by overcoming the problems caused by the waiting times caused by the satellite transit time. Especially with the GPS units to be installed in the deformation zones determined from the satellite data, the tracking process can be improved significantly.

This approach can enable real-time and continuous deformation monitoring, especially at mine sites, which can lead to a more comprehensive understanding of ground motions at mine sites. Since the method requires minimum field application, it will stand out as an approach that takes occupational health and safety into account at the highest level.

ACKNOWLEDGEMENT

The authors would like to thank Prof. Dr. Kemal Özgür Hastaoğlu, who works at Sivas Cumhuriyet University, Faculty of Engineering, Survey Engineering, for his support. The authors would like to thank the Kangal Coal Enterprise officials for their cooperation and Geomine R & D company for MineSAR software support.

REFERENCES

- [1] Hastaoğlu, K. Ö., Gül, Y., Poyraz, F., and Kara, B. C. (2019). Monitoring 3D areal displacements by a new methodology and software using UAV photogrammetry. *International Journal of Applied Earth Observation and Geoinformation*, 83, 101916.
- [2] Poyraz, F., Gül, Y., and Duymaz, B. (2020). Determination of deformations by using the PSI technique at a common dump site of three different open-pit marble mines in Turkey. *Turkish J. Earth Sci.* 29, 1004–1016.
- [3] Hastaoğlu, K.O. (2016). Comparing the results of PSInSAR and GNSS on slow motion landslides, Koyulhisar, Turkey. *Geomatics, Nat. Hazards Risk* 7, 786–803
- [4] Carlà, T., Tofani, V., Lombardi, L., Raspini, F., Bianchini, S., Bertolo, D., Thuegaz, P., and Casagli, N. (2019). Combination of GNSS, satellite InSAR, and GBInSAR remote sensing monitoring to improve the understanding of a large landslide in high alpine environment. *Geomorphology* 335, 62–75.
- [5] Poyraz, B. (2023). Maden işletmelerinde yüzey deformasyonlarının yapay açıklıklı uydu radar görüntüleriyle izlenebilirliğinin araştırılması. (Tez No. 802631) [Doktora Tezi, Sivas Cumhuriyet Üniversitesi], Yükseköğretim Kurulu Tez Merkezi (in Turkish), Sivas.
- [6] Casu, F., Manzo, M., and Lanari, R. (2006). A quantitative assessment of the SBAS algorithm performance for surface deformation retrieval from DInSAR data. *Remote Sens. Environ.* 102, 195–210.

- [7] Ferretti, A., Savio, G., Barzaghi, R., Borghi, A., Musazzi, S., Novali, F., Prati, C., and Rocca, F. (2007). Submillimeter accuracy of InSAR time series: Experimental validation. *IEEE Trans. Geosci. Remote Sens.*, 45, 1142–1153
- [8] Fuhrmann, T., Garthwaite, M., Lawrie, S., and Brown, N. (2018). Combination of GNSS and InSAR for future Australian datums. In: *IGNSS Symposium 2018 - International Global Navigation Satellite Systems Association*, pp. 1–13.
- [9] Poyraz, F., and Hastaoğlu, K.O. (2020). Monitoring of tectonic movements of the Gediz Graben by the PSInSAR method and validation with GNSS results. *Arab. J. Geosci.*, 13, 1–11.
- [10] Bányai, L., Bozsó, I., Szűcs, E., Gribovszki, K., and Wertzergom, V. (2023). Monitoring strategy of geological hazards using integrated three-dimensional InSAR and GNSS technologies with case study. *Period. Polytech. Civ. Eng.*
- [11] Rovira-Garcia, A., Juan, J.M., Sanz, J., González-Casado, G., and Ibáñez, D. (2016). Accuracy of ionospheric models used in GNSS and SBAS: methodology and analysis. *J. Geod.*, 90, 229–240.
- [12] Del Soldato, M., Confuorto, P., Bianchini, S., Sbarra, P., and Casagli, N. (2021). Review of works combining GNSS and InSAR in Europe. *Remote Sens.* 13, 1684.
- [13] Hu, B., Chen, J., and Zhang, X. (2019). Monitoring the land subsidence area in a coastal urban area with InSAR and GNSS. *Sensors* 19, 3181.
- [14] Parizzi, A., Gonzalez, F.R., and Brcic, R. (2020). A covariance-based approach to merging InSAR and GNSS displacement rate measurements. *Remote Sens.* 12, 300.
- [15] Pawluszek-Filipiak, K., and Borkowski, A. (2020). Integration of DInSAR and SBAS techniques to determine mining-related deformations using Sentinel-1 Data: The case study of Rydułtowy Mine in Poland. *Remote Sens.* 2020, Vol, 12, Page 242 12, 242.
- [16] Kim, J., Lin, S.Y., Singh, R.P., Lan, C.W., and Yun, H.W. (2021). Underground burning of Jharia coal mine (India) and associated surface deformation using InSAR data. *Int. J. Appl. Earth Obs. Geoinf.* 103, 102524.
- [17] Gül, Y. (2006). Bazı açık işletmelerdeki değişik kaya birimlerinin taşıma kapasitelerinin araştırılması ve kayaç özellikleri ile ilişkilendirilmesi. (Tez No. 181739) [Doktora Tezi, Sivas Cumhuriyet Üniversitesi], Yükseköğretim Kurulu Tez Merkezi (in Turkish), Sivas.
- [18] Sandwell, D., Mellors, R., Tong, X., Wei, M., and Wessel, P. (2011). Open radar interferometry software for mapping surface deformation. *Eos, Trans. Am. Geophys. Union* 92, 234–234.
- [19] Sandwell, D., Mellors, R., Tong, X., Xu, X., Wei, M., and Wessel, P. (2016). GMTSAR: An InSAR processing system based on generic mapping tools (second edition). Scripps institution of oceanography technical report. Livermore, CA (United States).

- [20] Hooper, A., Bekaert, D., Hussain, E., and Spaans, K. (2018). StaMPS/MTI manual version 4.1b. School of Earth and Environment University of Leeds, United Kingdom.
- [21] Arikan, M., Hooper, A., and Hanssen, R. (2010). Radar time series analysis over west Anatolia. In: Lacoste Francis H (editor). Fringe 2009 Proceedings. ESA SP 677. Noordwijk, Netherlands: ESA, pp. 1-6.
- [22] Fuhrmann, T., and Garthwaite, M. C. (2019). Resolving three-dimensional surface motion with InSAR: Constraints from multi-geometry data fusion. *Remote Sensing*, 11(3), 241. <https://doi.org/10.3390/rs11030241>
- [23] Hanssen, R.F. (2001). Radar interferometry: Data interpretation and error analysis. *Remote Sensing and Digital Image Processing*. Springer Dordrecht, Dordrecht.
- [24] Brouwer, W. (2021). An analysis of the InSAR displacement vector decomposition: InSAR fallacies and the strap-down solution. Delft University of Technology. Master thesis, 140pp, Netherlands
- [25] Bektaş, S. (2005). Endirekt ve koşullu ölçülerle dengeleme hesabı. OMÜ yayınlari, Yayın No:118, ISBN 975- 7636-54-1, 208 sayfa, OMÜ Basımevi,
- [26] <https://webapp.csrscs.nrcan-rncan.gc.ca/geod/tools-outils/ppp.php?locale=en> (accessed date: 7.11.23).
- [27] Bayık, Ç. (2018). Çok zamanlı ve çok frekanslı SAR-GNSS verileri ile heyelanların araştırılması: Beylikdüzü-Esenyurt örneği. Bülent Ecevit Üniversitesi; Fen Bilimleri Enstitüsü (Doktora Tezi); 137s; Zonguldak
- [28] Çınar, O. (2019). Yapay açıklıklı radar ve GPS/GNSS verileri ile düşey yönlü yüzey deformasyonlarının modellenmesi. Çanakkale Onsekiz Mart Üniversitesi, Fen Bilimleri Enstitüsü (Yüksek Lisans Tezi), 91s, Çanakkale
- [29] Cigna, F., Esquivel Ramírez, R., and Tapete, D. (2021). Accuracy of Sentinel-1 PSI and SBAS InSAR displacement velocities against GNSS and geodetic leveling monitoring data. *Remote Sensing*, 13(23), 4800.